Volume 1 | Number 1 | Jan 2013 | Pages 1–100

PCCP

Physical Chemistry Chemical Physics
www.rsc.org/pccp

ROYAL SOCIETY OF CHEMISTRY

This is an *Accepted Manuscript*, which has been through the Royal Society of Chemistry peer review process and has been accepted for publication.

Accepted Manuscripts are published online shortly after acceptance, before technical editing, formatting and proof reading. Using this free service, authors can make their results available to the community, in citable form, before we publish the edited article. We will replace this *Accepted Manuscript* with the edited and formatted *Advance Article* as soon as it is available.

You can find more information about *Accepted Manuscripts* in the **Information for Authors**.

Please note that technical editing may introduce minor changes to the text and/or graphics, which may alter content. The journal's standard **Terms & Conditions** and the **Ethical guidelines** still apply. In no event shall the Royal Society of Chemistry be held responsible for any errors or omissions in this *Accepted Manuscript* or any consequences arising from the use of any information it contains.

Journal Name

ARTICLE TYPE

Investigation of Fickian diffusion in the ternary mixtures of water-ethanol-triethylene glycol and its binary pairs

J.C. Legros[a], Y. Gaponenko[a,b], A. Mialdun[a], T. Triller[c], A. Hammon[c], C. Bauer[c], W. Köhler[c] and V. Shevtsova[*a]

We present a comprehensive experimental study of isothermal Fickian diffusion in the ternary and binary liquid mixtures of water, ethanol, and triethylene glycol over the entire ternary composition space. 21 ternary mixtures inside the composition triangle have been investigated by means of the Taylor dispersion technique and 30 binary mixtures by Taylor dispersion and/or optical beam deflection in a Soret cell. The scalar binary diffusion coefficient has been determined along all three binary boundaries of the composition space and compared with estimations based on the Stokes-Einstein relation using stick or slip boundary conditions. The four elements of the ternary diffusion matrix and the diffusion eigenvalues were determined over a large portion of the composition triangle. The pseudo-binary diffusion coefficients obtained in Taylor dispersion experiments with either one of the two independent concentrations kept constant are comparable to the two diffusion eigenvalues. One of the two off-diagonal elements of the diffusion matrix is of the same order as the diagonal ones and, hence, not negligible, whereas the other one is approximately one order of magnitude smaller. Where available, our results compare well with literature data. The investigated compositions also comprise the five compositions that are scheduled for microgravity experiments in the ESA DCMIX$_3$ project.

1 Introduction

Multicomponent diffusion is ubiquitous in nature, and the knowledge of diffusion coefficients in liquids is of great importance for applications in chemical engineering, separation science, microfluidics and others. In processes where diffusion occurs simultaneously with other phenomena, such as chemical reactions or phase transitions, it limits the overall rate of the process. The necessity for a precise knowledge of diffusion coefficients is high.

Numerous experimental techniques have been developed for the measurement of diffusion in binary mixtures and reliable experimental data are available for many binary systems[1]. The often used techniques comprise isothermal methods dedicated to diffusion (Taylor dispersion[2,3], interferometry[4,5], sliding cells[6], etc) and non-isothermal approaches aimed at simultaneous determination of diffusion and thermodiffusion (also called thermal diffusion) coefficients[7–12]. Nowadays, experimentally determined multicomponent diffusion coefficients are only available

for a limited number of ternary and higher mixtures[13]. Multicomponent diffusion is more complicated than it is often realized. For example, a ternary system has four diffusion coefficients, instead of one in a binary mixture. Furthermore, the values of diffusion coefficients in ternary mixtures depend on the order of the components as well as on the frame of reference for which the diffusive fluxes are written. Only the eigenvalues of the diffusion matrix are invariant with respect to the order of the components and the frame of reference. The binary diffusion coefficient does not depend on the frame of reference.

Diffusion coefficients quantify the proportionality constant between diffusion fluxes and composition gradients. The Fickian diffusion fluxes can be expressed based on various velocity reference frames: molar-, mass-, and volume-average velocity[14]. The mathematical model of Taylor dispersion technique was originally developed for the volume-average reference frame[15]. Then the molar diffusion fluxes in a ternary mixture can be written as

$$J_1 = -(D_{11}\nabla C_1 + D_{12}\nabla C_2) , \tag{1}$$

$$J_2 = -(D_{21}\nabla C_1 + D_{22}\nabla C_2) , \tag{2}$$

where C_i is the molar concentration of component i and D_{ij}

[a] Microgravity Research Center, Université Libre de Bruxelles (ULB), CP–165/62, Av. F.D. Roosevelt, 50, B–1050 Brussels, Belgium. E-mail: vshev@ulb.ac.be
[b] Institute of Computational Modelling SB RAS, Krasnoyarsk, 660036, Russia
[c] Physikalisches Institut, Universität Bayreuth, D-95440 Bayreuth, Germany. E-mail: werner.koehler@uni-bayreuth.de

denotes the matrix of Fickian diffusion coefficients of size $(n-1)^2$. The third component, which does not appear explicitly in eqns (1)-(2) as well as in the diffusion equations below, can be evaluated using the condition of zero volume flow

$$J_1 V_{1m} + J_2 V_{2m} + J_3 V_{3m} = 0 \ .$$

Here, V_{im} is the partial molar volume of component i.

In molecular dynamics simulations the use of molecular mass is appropriate for the numbering of the components. Hydrodynamic effects become important when liquid mixtures are studied on a macroscopic scale. Correspondingly, it is appropriate to choose the numbering of the component according to the density: water (component 1), ethanol (component 2) and triethylene glycol (component 3).

Two independent components in a ternary mixture require an experimental set-up with two independent diagnostics[16] and measurements become more laborious than in binaries. In addition to this, the data processing is also more complex and often results in large uncertainties[17]. Furthermore, in those cases where more than one data point exists, often measurements by different experimental groups quite often agree only for the eigenvalues of the diffusion matrix but not for its individual elements[18–20].

In addition to industrial applications, reliable experimental data on ternary diffusion are needed for elucidating some fundamental questions still under discussion, like the relation between the eigenvalues of the diffusion matrix and the quasi-binary diffusion coefficient[21] or the sign of the main diffusion coefficients D_{11} and D_{22}[13].

Our current interest in examining diffusion in multicomponent systems is also motivated by its importance for the interpretation of thermodiffusion experiments. Thermodiffusion accounts for a concentration separation in a liquid mixture in response to an imposed temperature gradient. The measurement of thermodiffusion in ternary mixtures causes serious difficulties both from the experimental and the mathematical sides. While using two wavelength techniques, the transient behavior of the ternary system depends on four mass diffusion and two Soret coefficients to be determined. It turns out that six parameters fitting is subjected to large errors and the coefficients cannot be determined reliably[22]. Prior knowledge of mass diffusion coefficients can dramatically decrease the complexity of the determination of thermodiffusion and Soret coefficients.

It is worth noting that in the framework of the European Space Agency (ESA) program DCMIX (Diffusion and Thermodiffusion Coefficients Measurements in Ternary Mixtures), the research groups conduct experiments on board the International Space Station[23–25] (ISS) to validate ground experimental techniques and various theories. Accordingly, this study was also motivated by the preparation of the experiment DCMIX$_3$ on the ISS with the mixture water-ethanol-triethylene glycol. The experiment on the ISS will be coordinated by the group of Köhler in Bayreuth (Germany), and the MRC group has measured mass diffusion coefficients with the purpose to determine the relaxation time and the duration of the experiment on the ISS.

We use the Optical Beam Deflection (OBD) and Taylor disper-
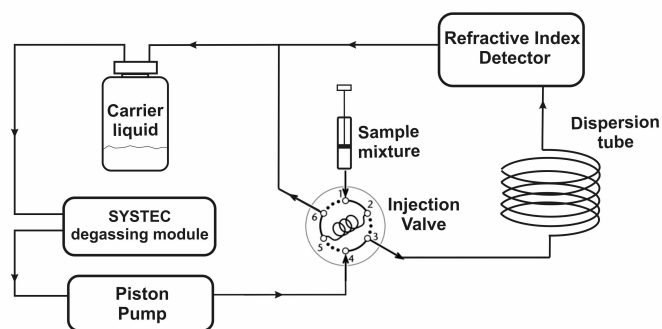
Fig. 1 Sketch of the set-up used in Taylor dispersion technique

sion techniques for measurements of binary and ternary coefficients. Although the main target is the analysis of ternary mixtures, the knowledge of the three binary subsystems is very important for the underlying asymptotic behavior on approach of the binary limits. Of course, some of the difficulties encountered when extracting several parameters from a limited set of experimental data in thermodiffusion experiments on ternary mixtures[17] are also present in case of isothermal diffusion[18]. Nevertheless, the situation is somewhat easier due to the absence of temperature gradients, and the obtained here isothermal diffusion coefficients can later advantageously be employed for the interpretation of thermodiffusion experiments on ternary mixtures.

2 Experimental section

2.1 Taylor Dispersion technique

2.1.1 Working principle and instrument

The Taylor dispersion technique was used for measurements of binary and ternary diffusion coefficients. When a carrier solution is pumped through a long capillary tube, the laminar profile for Newtonian fluids has a parabolic velocity distribution. A small volume of the same solution with a slightly different composition is injected. The flow of the carrier fluid disperses this volume, and also induces radial composition gradients which in turn cause radial diffusion. Diffusive fluxes also occur at the front and back sides of the injected volume. These fluxes become important if the radial diffusive fluxes are roughly of the same order of magnitude as the convective axial fluxes. This is the case when either the axial velocity is very low, or when the radial distances are very small. Under the action of convection and diffusion, the axial distribution of the concentration in the injected volume takes the form of a Gaussian peak. At the end of the capillary a differential refractometer monitors the change in the concentration profile. The Fickian diffusion coefficient is calculated from the resulting profile of the refractive index variation. The sketch of the Taylor dispersion set-up used in this and previous studies[18,27] is shown in Fig. 1.

To satisfy the theoretical assumptions[15], Taylor dispersion experiments are usually carried out in capillaries with a small diameter. A Teflon (PTFE) tube of a length of $L = (29.839 \pm 0.001)$ m with a circular cross-section of radius $R_0 = 374\,\mu$m was used. The

capillary was coiled around a grooved aluminum cylinder with a diameter of 30 cm and was placed in a temperature-regulated air bath. A HPLC analytical pump (Knauer S1000) with active pulsation damping was used to push the carrier solution through the dispersion tube. The utilized Knauer Smartline RI Detector 2300 ($\lambda = 950$ nm) is suited for recording small concentration variations by its differential sensitive refractometer. To prevent bubbles from disturbing the flow, the SYSTEC degassing module is installed and connected in-line before the pump. The flow rate during the measurements was 0.08 mL/min. Zero dead volume fittings were used to connect the capillary with the six port injection valve with injection volume $\Delta V = 20\,\mu$L. The RI detector and the dispersion tube were kept in the same air bath at a constant temperature of 298 ± 0.2 K. The detector was connected to a computer for digital data acquisition using the Clarity Software by DataApex. The basic tests and validation of the experimental set-up with binary mixture were presented previously[27].

2.1.2 Experimental procedure

Fickian diffusion coefficients were measured in 21 ternary and 30 binary mixtures which are shown in Fig. 2. The following substances from Acros Organics were used without further purification: water pure, deionized reagent Grade 3 (CAS Number: 7732-18-5); triethylene glycol 99%(CAS Number: 112-27-6) and from VWR, ethanol absolute for analytical reagent grade, (CAS Number: 64-17-5). To prepare ternary mixtures poor in water (e.g., point 15), very energetic and long shaking of the vial was required. A similar observation has been reported by Klein&Wiegand[7] while performing experiments in binary mixtures of glycols in ethanol; they have found a drastic decrease of solubility with increasing chain length of the glycols.

The carrier (200 g) and injected (20 g) solutions were prepared gravimetrically with an accuracy of ± 0.005 g. For the ternary mixtures three different pulse samples, each of them 20 g, were prepared by weighing. The composition difference between the carrier and injected pulse solution was kept below 0.05 g/g (relative difference). The carrier liquid was allowed to flow through the Taylor apparatus for at least one day to ensure a stationary base line. The pulse solutions were then injected into the carrier flow. Every four-five hours after an injection, a new sample was injected into the carrier. The time between two successive injections was chosen such that a new injection was done only after recording and visual analysis of the previous peak. Each pulse solution was injected at least three times. Hence, a total of nine or more measurements were carried out for each studied composition. When the carrier solution was exchanged, the apparatus was flushed two or more times (depending on the composition) with a new solution at a flow rate of 0.5 mL/min. After each cycle, the used 30 mL of liquid were disposed. At the next step, 60 mL of fresh solution were allowed to run overnight at the operating flow rate. Then once again, the carrier liquid was replaced by 100 mL of the fresh solution and it was allowed to flow one to two days for equilibration before the first injection.
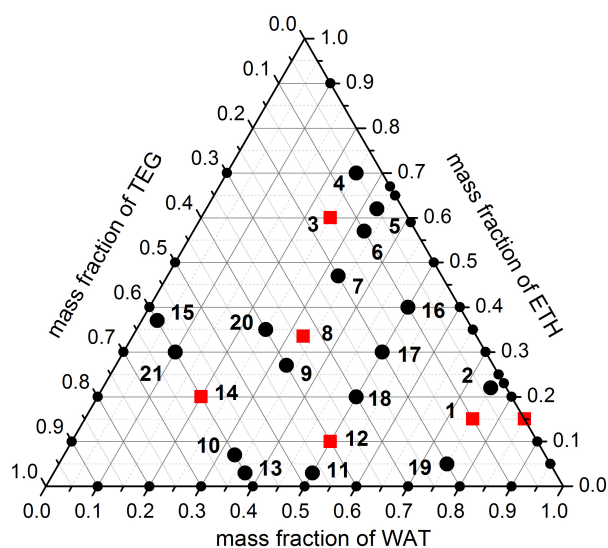
Fig. 2 Concentration matrices in mass fractions. The circles show the concentrations at which the Fickian diffusion coefficients have been measured in the ternary mixture water+ethanol+triethylene glycol (21 points) and its subsystems (30 points). The red squares indicate the points at which thermodiffusion experiments will be carried out on the ISS.

2.1.3 Sensitivity of the Taylor set-up detector

Diffusion coefficients can be determined from the experiment by fitting experimental points to the solution for the concentration distributions. We do not measure concentration C_i (mol/m^3) directly, instead, we measure an electrical signal in mV which is related to a refractive index variation. The detector voltage output signal $V(t)$ is assumed to be linearly dependent on the concentration change of the flow[30]

$$V(t) = \sum_{i=0}^{N} \gamma_i t^i + [R_1(C_1(t) - C_1^0)] + [R_2(C_2(t) - C_2^0)] \qquad (3)$$

here $R_i = \partial V/\partial C_i$ is the sensitivity of the detector to the i-th component of the mixture. When measuring very small concentration differences, even a small drift of the baseline causes inaccuracies in the final results and has to be subtracted from the raw signals. The baseline drift of the detector (first term in eqn (3) was modeled using a polynomial fit of order N, usually $N = 2$.

The sensitivity R_i can be defined in two ways: by current measurements or from independent measurements of contrast factors. If the variation of the refractive indices with concentration, $\partial n/\partial C_i$, (called contrast factors) are known for the wavelength of the detector, then

$$R_i = \partial V/\partial C_i = (\partial V/\partial n)(\partial n/\partial C_i)$$

where $(\partial V/\partial n)$ is the constant of the detector. However, the contrast factors at wavelength $\lambda > 900$ nm are available only for a limited number of ternary mixtures[31–33].

Alternatively, the sensitivity R_i can be determined during the Taylor dispersion experiment. The surface area between the dispersion peak and the baseline can be calculated as

$$S = \int_{t_1}^{t_2} \left(V(t) - \sum_{i=0}^{N} \gamma_i t^i \right) dt = R_1 \int_{t_1}^{t_2} \left(C_1(t) - C_1^0 \right) dt + R_2 \int_{t_1}^{t_2} \left(C_2(t) - C_2^0 \right) dt \tag{4}$$

The area of the peak measured by the refractometer is equal to the one just after injection. The excess concentration ΔC_i of the each component within the pulse is uniform just after injection. Considering that the time interval during which the initial 'rectangular' pulse ΔC_i flows through the capillary cross-section is $\Delta t = \Delta V/q$, the following relation holds:

$$\int_{t_1}^{t_2} \left(C_i(t) - C_i^0 \right) dt = \Delta C_i \Delta t = \Delta C_i \frac{\Delta V}{q} . \tag{5}$$

Here, ΔV is the injected volume and q is the flow rate of the carrier liquid. Thus eqn (4) can be written as

$$S \frac{q}{\Delta V} = R_1 \Delta C_1 + R_2 \Delta C_2 . \tag{6}$$

Performing two experiments with different injected compositions, ΔC_i results in a system of linear equations:

$$S^1 \frac{q}{\Delta V} = R_1 \Delta C_1^1 + R_2 \Delta C_2^1 \tag{7}$$

$$S^2 \frac{q}{\Delta V} = R_1 \Delta C_1^2 + R_2 \Delta C_2^2 . \tag{8}$$

Here, the superscripts denote the test number, the subscripts denote the component number and S^i is the measured area under the peak. The solution of this system of linear equations provides the sensitivity ratio

$$S_R = \frac{R_1}{R_2} = \frac{\Delta C_2^2 \, S^1 - \Delta C_2^1 \, S^2}{\Delta C_1^1 \, S^2 - \Delta C_1^2 \, S^1} \tag{9}$$

using the peak areas measured in two tests. This approach does not require a specific order of injections and, correspondingly, the requirement[28] that first two injections have to be done while one of the compositions does not change ($\Delta C_1^2 = 0$ or $\Delta C_2^1 = 0$) can be omitted.

2.1.4 Basic equations

Here, we shortly describe the mathematical approach for ternary mixtures. For binary mixtures it can be obtained in a similar way or it can easily be found in the literature[1]. Equations for the concentration profile are derived in a moving frame of reference instead of the laboratory fixed one. Thus the concentration distribution of the injected pulse is measured relative to an axial coordinate z moving with the mean velocity U_0. Assuming that diffusion coefficients are constant during the experiment and no volume changes occur on mixing, the mathematical description of a concentration profile for a ternary mixture is given by[29]

$$\frac{\partial C_i}{\partial t} + U_0 \left(1 - 2\frac{r^2}{R^2}\right)\frac{\partial C_i}{\partial z} = \sum_{j=1}^{2} D_{ij}\left(\frac{\partial^2 C_j}{\partial z^2} + \frac{\partial^2 C_j}{\partial r^2} + \frac{1}{r}\frac{\partial C_j}{\partial r}\right).$$

$$(i, j = 1,2) \quad (10)$$

Here C_i is the molarity of the component i, D_{ij} are the Fickian diffusion coefficients; r and z are the radial and axial coordinates,

respectively. Under a set of assumptions, the solution of eqn (10) for the time dependences of radially averaged concentrations of the dispersed components at the outlet of the tube was obtained in the analytical form[3,29]

$$C_i(t) - C_i^0 = \frac{2\Delta V}{R^3 U_0}\sqrt{\frac{3}{\pi^3 t}}\left(A_{i1}\sqrt{\hat{D}_1}\exp(-\hat{D}_1 \eta) + \right.$$

$$\left. A_{i2}\sqrt{\hat{D}_2}\exp(-\hat{D}_2 \eta)\right), \tag{11}$$

where η is the abbreviation for $12(t - t_R)^2/R^2 t$; C_1^0 is the molarity of the carrier liquid; ΔV is the volume of the injected solution sample. The eigenvalues $\hat{D}_i$ of the diffusion matrix D_{ij} are defined as

$$\hat{D}_1 = \frac{D_{11} + D_{22} + \sqrt{(D_{11} - D_{22})^2 + 4D_{12}D_{21}}}{2} \tag{12}$$

$$\hat{D}_2 = \frac{D_{11} + D_{22} - \sqrt{(D_{11} - D_{22})^2 + 4D_{12}D_{21}}}{2} \tag{13}$$

and the coefficients A_{ik} are defined as

$$A_{11} = \frac{(D_{22} - \hat{D}_1)\Delta C_1 - D_{12}\Delta C_2}{\hat{D}_2 - \hat{D}_1} \tag{14}$$

$$A_{12} = \frac{(D_{22} - \hat{D}_2)\Delta C_1 - D_{12}\Delta C_2}{\hat{D}_1 - \hat{D}_2} \tag{15}$$

$$A_{21} = \frac{(D_{11} - \hat{D}_1)\Delta C_2 - D_{21}\Delta C_1}{\hat{D}_2 - \hat{D}_1} \tag{16}$$

$$A_{22} = \frac{(D_{11} - D^{(2)})\Delta C_2 - D_{21}\Delta C_1}{\hat{D}_1 - \hat{D}_2} \tag{17}$$

ΔV enters into eqn (11) because the coefficients A_{ik} originally include the excess number of moles present in the solute in the injected volume ΔV: $\Delta n_1 = \Delta C_1 \Delta V$.

2.1.5 Concentration units

The mixtures in our experiments were prepared using mass fractions and the contrast factors were previously measured also using mass fractions. However the original equations (10) and their solutions (11) obtained with numerous assumptions were written in molar concentration (moles of solute per liter of solution).

The concentration in mass fraction c_i is expressed via the molar concentration C_i as

$$c_i = C_i \frac{M_i}{\rho} \quad \text{or vise versa} \quad C_i = c_i \frac{\rho}{M_i} . \tag{18}$$

Here, M_i is the molar mass of the constituent i and ρ is the density of the mixture.

Then, the coefficients A_{ik} in different units will be written as

$$A_{ik} = f(C_i, D_{ij}, \hat{D}_1, \hat{D}_2) = \rho f(\frac{c_i}{M_i}, D_{ij}, \hat{D}_1, \hat{D}_2) .$$

For the sensitivities R_i the change of variables will give

$$R_i = \frac{\partial V}{\partial c_i}\frac{\partial c_i}{\partial C_i} = \frac{\partial V}{\partial c_i}\frac{M_i}{\rho} = \frac{\partial V}{\partial n}\frac{M_i}{\rho}\frac{\partial n}{\partial c_i} \ . \tag{19}$$

Below, only the ratio of sensitivities S_R will be used. In the case where contrast factors are known and they were measured using mass fraction, S_R will be written as

$$S_R = \frac{R_1}{R_2} = \frac{\partial V/\partial C_1}{\partial V/\partial C_2} = \frac{M_1}{M_2}\frac{\partial n/\partial c_1}{\partial n/\partial c_2}. \tag{20}$$

In the case when S_R should be determined from the Taylor experiment, eqn (9) in a new variable will take form

$$S_R = \frac{M_1}{M_2}\frac{\Delta c_2^2\, S^1 - \Delta c_2^1\, S^2}{\Delta c_1^1\, S^2 - \Delta c_1^2\, S^1} \ . \tag{21}$$

2.2　Optical Beam Deflection

2.2.1　Experimental setup

The technique used in Bayreuth for measuring transport coefficients (Fickian and Soret diffusion) is Optical Beam Deflection with a single wavelength for binary systems[10,37,38]. It relies on changes of the refractive index, which accompany concentration changes in a sample. The sample is contained between two copper plates inside a glass frame, which constitute a diffusion cell with $l = 1$ cm length and a height of $h = 1.43$ mm. Peltier elements allow to apply a well defined temperature gradient along the z-direction of the cell. By measuring the deflection δz of a laser beam (637 nm) passing through this cell by means of a line camera (at distance $l_d = 1.32$ m from the cell), the temporal evolution of the refractive index gradient is recorded:

$$\delta z = l\langle\frac{\partial n}{\partial z}\rangle\left(\frac{l}{2n} + \frac{l_w}{n_w} + \frac{l_d}{n_{air}}\right) \ . \tag{22}$$

Here, n is the refractive index of the sample and n_{air} the refractive index of air. l_w and n_w are parameters of the glass frame. $\langle\partial n/\partial z\rangle$ denotes the average of the refractive index gradient over the gaussian beam profile. Fig. 3 shows a typical ODB signal. There are two contributions to $\langle\partial n/\partial z\rangle$: a thermal change $(\partial n/\partial T)_{p,c}$ and a concentration change $(\partial n/\partial c)_{p,T}$:

$$\frac{\partial n}{\partial z} = \left(\frac{\partial n}{\partial T}\right)_{p,c}\frac{\partial T}{\partial z} + \left(\frac{\partial n}{\partial c}\right)_{p,T}\frac{\partial c}{\partial z} \tag{23}$$

$(\partial n/\partial T)_{p,c}$ and $(\partial n/\partial c)_{p,T}$ are the contrast factors. $(\partial n/\partial c)_{p,T}$ is obtained from a concentration series of the refractive index, which is measured by means of a refractometer (Anton Paar Abbemat WR-MW). $(\partial n/\partial T)_{p,c}$ is measured interferometrically[34,35]. Both techniques are documented in the literature[8,10,20].

To extract the transport coefficients from the OBD signal, the heat equation and extended diffusion equation

$$\partial_t T = D_{th}\nabla^2 T \tag{24}$$

$$\partial_t c = D\nabla^2 c + D_T c(1-c)\nabla^2 T \tag{25}$$

are solved numerically. The temperatures inside the copper plates are measured with thermistors and used as time-dependent
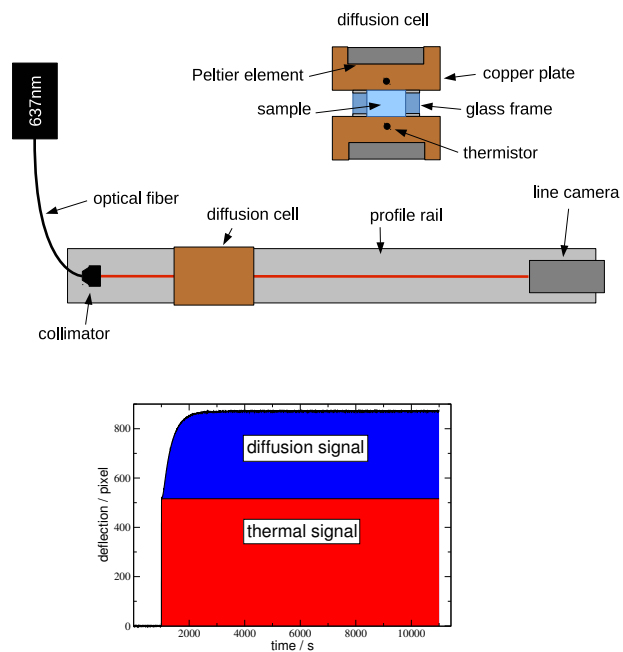
Fig. 3 Top: Schematics of the OBD setup and the diffusion cell. Bottom: A typical OBD signal. The first rise is mainly due to the thermal contrast factor $(\partial n/\partial T)_{p,c}$. Because mass diffusion happens on longer time scales, one can separate the contributions due to $(\partial n/\partial c)_{p,T}$.

boundary conditions.

The OBD technique has been used for new measurements of the diffusion coefficients of the binary systems water-TEG and ethanol-TEG and for previous measurements of water-ethanol mixtures by the Bayreuth group[10], which are also referenced together with the new results.

We have also tried to compare our data with theoretical estimations of the tracer diffusion coefficients in the dilute limits. The most basic model is the Stokes-Einstein equation

$$D = \frac{k_B T}{n\pi\eta R_0} \ , \tag{26}$$

where the solute is treated as a sphere of radius[36]

$$R_0 = \left(0.64 \times \frac{3M_t}{4\pi N_A \rho_t}\right)^{1/3} \tag{27}$$

that experiences a hydrodynamic friction in a solvent continuum of viscosity η. Here, ρ_t is the density and M_t the molar mass of the solute (tracer), N_A is Advogadro's number, and $k_B T$ is the thermal energy. The factor n accounts for the proper boundary conditions. In case of diffusing particles that are significantly larger than the solvent molecules, stick boundary conditions with $n = 6$ are appropriate. It has been found that eqn 26 works surprisingly well even down to the molecular scale, provided that slip boundary conditions, corresponding to $n = 4$, are used, if the solute molecules are comparable to or smaller than the solvent molecules[36,43].

The Stokes-Einstein model is based on a simple physical picture, which makes it appealing. However, being a hydrodynamic

model, it cannot account for molecular details and, in particular, not for association. Significant work has been undertaken to obtain better correlations for diffusion coefficients in dilute solution. An overview over different models discussed in the literature has been compiled by Mutoru et al. [46], who have investigated diffusion of carbon dioxide in water. An empirical correlation that can be used both for associating and non-associating liquids has been proposed by Wilke and Chang [47]:

$$D = 7.4 \times 10^{-8} \frac{(xM)^{1/2}T}{\eta V_t^{0.6}} \qquad (28)$$

Here, η and M are the viscosity and molar mass of the solvent, respectively. $V_t = M_t/\rho_t$ is the molar volume of the tracer. The association parameter x has been given in Ref. [47] for water ($x = 2.6$) and ethanol ($x = 1.5$). For triethylene glycol we have assumed $x = 1$. Larger values lead to poorer agreement with the experimental data. Table 1 summarizes the parameters used for the calculation of the tracer diffusion coefficients in the six dilute limits according to eqns (27) and (28). Note that cgs-units are used in eqn (28), which has been taken directly from Ref. [47], whereas SI-units are used otherwise throughout the paper.

Table 1 Parameters of liquids used for calculation of tracer diffusion coefficients according to eqns (26) and (28). Temperature $T = 298$ K.

		water	ethanol	triethyleneglycol
M	10^{-3} kg/mol	18	46	150
ρ	10^{-3} kg/m^3	1.00	0.79	1.12
η	mPa s	0.89	1.07	35.8

The tracer diffusion coefficients calculated from eqns (26) and (28) are summarized in table 2, and the data are also included in the plots for the binary diffusion coefficients. Generally, the agreement with the measured diffusion coefficients appears quite reasonable, with the measured data being somewhere in between the slip and the stick boundary condition. The Wilke and Chang model does not yield a better agreement than the simple Stokes-Einstein formula. For water as the minority component it is even significantly overestimates D by more than a factor of two.

Table 2 Diffusion coefficients for $c \to 1$ and $c \to 0$ calculated by the Stokes-Einstein equation (26) with slip and stick boundary conditions and according to Wilke and Chang (eqn. (28)) (in 10^{-10} m^{2}s^{-1}).

concentration	slip	stick	Wilke
water-ethanol, $c(\text{water}) \to 0$	18.4	12.3	30.2
water-ethanol, $c(\text{water}) \to 1$	15.0	10.0	14.8
water-triethylene glycol, $c(\text{water}) \to 0$	0.55	0.37	1.33
water-triethylene glycol, $c(\text{water}) \to 1$	11.4	7.6	9.0
ethanol-triethylene glycol, $c(\text{ethanol}) \to 0$	0.37	0.25	0.66
ethanol-triethylene glycol, $c(\text{ethanol}) \to 1$	9.4	6.3	9.1

3 Results and discussion

3.1 Binary mixtures

3.1.1 Water-ethanol

The diffusion coefficient of water-ethanol has already been measured with different experimental setups by various groups and
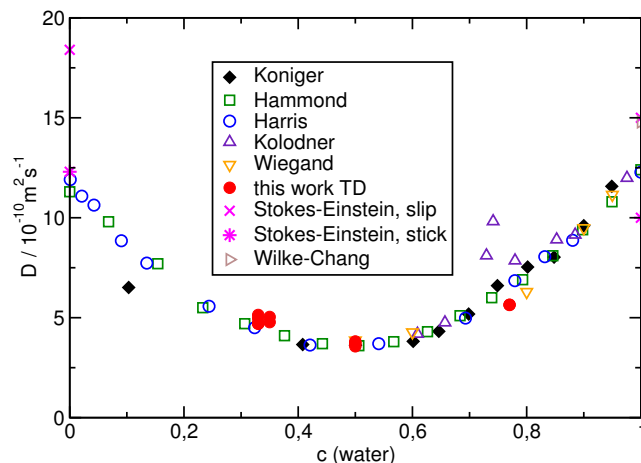
Fig. 4 Diffusion coefficient of water-ethanol at $T = 298$ K as a function of water mass fraction c. The theoretical value according to Wilke and Chang for $c(\text{water}) \to 0$ is off scale and has been omitted. Literature data by Königer (OBD) [10], Hammond (diaphragm cell) [39], Harris (Taylor dispersion) [40], Kolodner (OBD) [41], and Wiegand (thermal diffusion forced Rayleigh scattering) [42]. Note that the value for D at $c(\text{ethanol}) = 0.8968$ (corresponding to $c(\text{water}) = 0.1032$) has erroneously been listed as $D = 2.51 \times 10^{-10}$ m^{2}s^{-1} in table 3 of Ref. [10]. The correct value $D = 6.51 \times 10^{-10}$ m^{2}s^{-1} has, however, been plotted in Fig. 4 of Ref. [10].

allows to verify the presented techniques. Figure 4 shows literature data [39–42] together with OBD measurements [10] as well as new measurements using Taylor dispersion. As can be seen at the limits $c(\text{water}) \to 0$ and $c(\text{water}) \to 1$, the values estimated by the Stokes-Einstein equation (26) reproduce the measured data to within 25%, even though there is no clear preference for slip or stick boundary conditions. All measured values from different techniques give a coherent picture with good agreement. Notable deviations are only observed for a few data points measured by Kolodner and for the lowest concentration of Königer.

3.1.2 Water-triethylene glycol

The second investigated binary system is water-triethylengylcol. Table 3 and figure 4 summarize the results from Taylor dispersion and OBD measurements.

Table 3 Diffusion coefficients of water-triethylene glycol measured by OBD with different temperature gradients and the corresponding contrast factors. $T = 298$ K.

mass fr. water	ΔT	$\frac{\partial n}{\partial c}$	$\frac{\partial n}{\partial T}/10^{-4}$K^{-1}	$D/10^{-10}$m^{2}s^{-1}
0.30	-0.5K	-0.1229	-2.92	$2.25 \pm .10$
0.30	+0.5K	-0.1229	-2.92	$2.47 \pm .10$
0.50	-0.5K	-0.1305	-2.44	$3.92 \pm .25$
0.50	-1K	-0.1305	-2.44	$3.66 \pm .25$
0.50	+1K	-0.1305	-2.44	$4.19 \pm .25$
0.70	+0.5K	-0.1297	-1.81	$5.59 \pm .11$
0.70	+1K	-0.1297	-1.81	$5.37 \pm .11$

To demonstrate that the determined diffusion coefficients are not sensitive to the magnitude and sign of the temperature dif-

Table 4 Diffusion coefficients of water-triethylene glycol measured by Taylor Dispersion technique. $T = 298$ K.

mass fr. water	$D/10^{-10}\,\mathrm{m^2 s^{-1}}$
0.10	$1.58 \pm .03$
0.20	$1.89 \pm .05$
0.30	$2.42 \pm .01$
0.40	$3.14 \pm .05$
0.50	$3.81 \pm .07$
0.60	$4.75 \pm .02$
0.70	$5.46 \pm .03$
0.80	$6.28 \pm .07$
0.90	$7.14 \pm .05$

ference ΔT (provided the system shows no gravitational instabilities), we present results from measurements with different ΔT, both positive and negative. The largest deviation is observed at $c = 0.5$ for $\Delta T = -1K$ and $\Delta T = 1K$ and amounts to approx. 12%.

3.1.3 Ethanol-triethylene glycol

Table 5 and figure 6 show the results for the system ethanol-triethylene glycol measured with OBD. Again, the values calculated by the Stokes-Einstein equation provide a rough estimate for the diffusion coefficients in the dilute limits and correspond well with the measured data.

Table 5 Diffusion coefficients of ethanol-triethylene glycol measured by OBD and the corresponding contrast factors. $T = 298$ K.

mass fr. ethanol	$\frac{\partial n}{\partial c}$	$\frac{\partial n}{\partial T}/10^{-4}\,\mathrm{K^{-1}}$	$D/10^{-10}\,\mathrm{m^2 s^{-1}}$
0.10	-0.1088	-3.364	$1.10 \pm .02$
0.20	-0.1049	-3.444	$1.17 \pm .02$
0.30	-0.1019	-3.536	$1.82 \pm .04$
0.40	-0.0985	-3.621	$2.23 \pm .04$
0.50	-0.0950	-3.704	$2.83 \pm .06$
0.70	-0.0882	-3.865	$4.57 \pm .09$
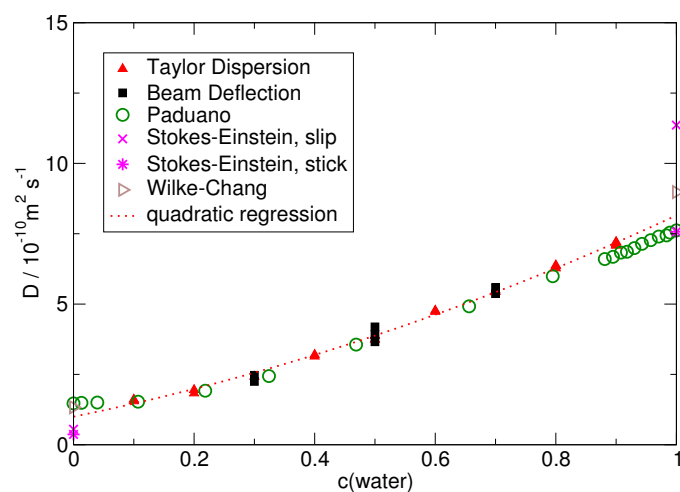
Fig. 5 Diffusion coefficient D of water-triethylene glycol as a function of water mass fraction. $T = 298$ K. Literature data from Paduano[48]
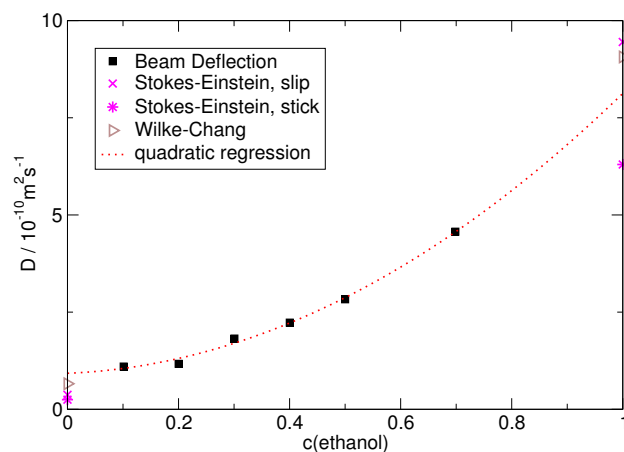
Fig. 6 OBD: Diffusion coefficient D of ethanol-triethylene glycol as a function of ethanol mass fraction at $T = 298$ K.

3.2 Ternary mixtures

We carried out only a limited number of experiments in ternary mixtures rich in ethanol and poor in water, (the upper part of triangle in Fig. 2) mainly due to unfavorable optical conditions. The contrast factors at the upper part of the triangle are small[31] and it may lead to a large uncertainty. The contrast factors even in a binary mixture of water-ethanol are small in this region[10]. Another reason is that one of the aims was to determine diffusion coefficients in the points of the future experiment on the ISS and they are absent in this region.

3.2.1 Fitting procedure

An unconstrained Nelder-Mead (simplex) method available in Matlab, similar to that employed by Mialdun *et al.*[18], was used for the fitting of experimental results with working equations. Instead of direct fitting of the coefficients D_{11}, D_{12}, D_{21} and D_{22} we have used the procedure suggested by Ray&Leaist[28]. A peak signal is normalized in a way that eqns (3), (11) take the form

$$V(t) = \sum_{i=0}^{N} \gamma_i t^i + \Delta V_{max} \sqrt{\frac{t_R}{t}} \left[W_1 exp(-\hat{D}_1 \eta) + (1 - W_1) exp(-\hat{D}_2 \eta) \right]$$

(29)

where W_1 is the normalized weight

$$W_1 = \frac{(a + b\alpha)\sqrt{\hat{D}_1}}{(a + b\alpha)\sqrt{\hat{D}_1} + (1 - a - b\alpha)\sqrt{\hat{D}_2}}$$

(30)

and the parameters a, b and α are

$$a = \frac{D_{11} - \hat{D}_1 - S_R D_{12}}{(\hat{D}_2 - \hat{D}_1)},$$

(31)

$$b = \frac{D_{22} - D_{11} - D_{21}/S_R + S_R D_{12}}{(\hat{D}_2 - \hat{D}_1)},$$

(32)

$$\alpha = \frac{\Delta c_1}{\Delta c_1 + \Delta c_2 (M_1/M_2)/S_R}.$$

(33)

Here Δc_1 and Δc_2 are the excess mass fractions in the injected solutions. The sensitivity ratio S_R is defined by eqns (20)-(21). In the fitting we used S_R obtained by measuring the refractive
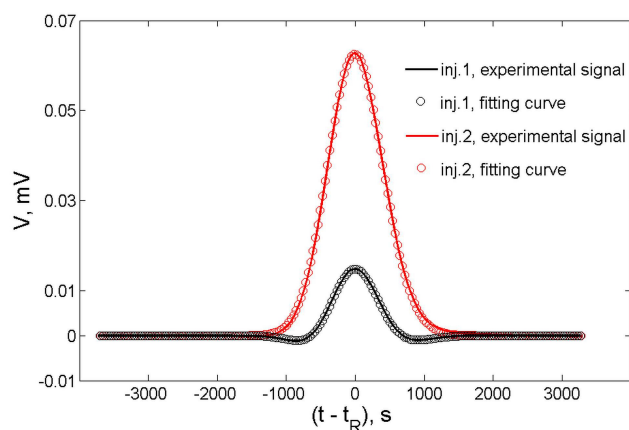
Fig. 7 Ternary dispersion profile (solid curves) and fitting curves (symbols) in ternary mixture water-ethanol-TEG corresponding to the point labeled 8: (injection 1) $\Delta c_1 = -0.030$, $\Delta c_2 = 0.030$; (injection 2) $\Delta c_1 = 0.030$, $\Delta c_2 = 0.00$. The base line for each experiment has been subtracted for clarity. $T = 298$ K.

Fig. 8 Ternary dispersion profiles with dips (solid curve) and fitting curve in ternary mixture water-ethanol-TEG corresponding to the point labeled 21; injection with $\Delta c_1 = -0.031$, $\Delta c_2 = 0.030$. The base line for each experiment has been subtracted for clarity. $T = 298$ K.

indices for $\lambda = 925$ nm by Sechenyh et al[31] and regularly carried out cross-checking using eqn (21). The used values of S_R are listed in Table 6. The described fitting procedure does not work in the case when $\hat{D}_1$ and $\hat{D}_2$ are equal.

The Fickian diffusion coefficients are calculated from the fit parameters $\hat{D}_1, \hat{D}_2, a$ and b as follows[28]:

$$D_{11} = \hat{D}_1 + \frac{a(1-a-b)}{b}(\hat{D}_1 - \hat{D}_2), \qquad (34)$$

$$D_{12} = \frac{1}{S_R}\frac{a(1-a)}{b}(\hat{D}_1 - \hat{D}_2), \qquad (35)$$

$$D_{21} = S_R\frac{(a+b)(1-a-b)}{b}(\hat{D}_2 - \hat{D}_1), \qquad (36)$$

$$D_{22} = \hat{D}_2 + \frac{a(1-a-b)}{b}(\hat{D}_2 - \hat{D}_1). \qquad (37)$$

Note, that there is a misprint with signs in eqn (32) in the original paper[28].

3.2.2 Some stratagems for data analysis

The determination of four diffusion coefficients D_{ij} by fitting is a notoriously difficult problem[17,18,25]. The most common obstacles are the following: multiple minima of the residual function, the dependence of final results on the initial guess, convergence to non-physical solution, or fitting leads to equal eigenvalues what is erroneous.

The latter deception can be avoided by analyzing the peak shape. Three types of peaks were observed in the considered mixtures. The Gaussian type peak shown in Fig. 7 (injection 2, $\Delta c_2 = 0$) can be positive or negative depending on the sign of Δc_1. Injection with another composition into the same carrier liquid may lead to a dispersion peak surrounded by two dips (Fig. 7, injection 1) and this peak was dubbed as "unusual" in previous works with diluted ternary mixtures[1,3]. However, for the water-ethanol-TEG mixture this shape of the peak is "usual" and it was noticed in 60% of the ternary points.

The observed dips were as small as in Fig. 7 or larger than in

Fig. 8 or even equal to the height of the central peak. The third shape was observed only in the points labeled 1 and 19 and it is characterized by the broadening and even small splitting of the Gaussian type peak at the top. The points at which dips were not found can be seen later in Fig. 10 marked by green triangles. The important point is that the emergence of peaks with a shape different from Gaussian type indicates that the eigenvalues of the system are different. This prevents selection of erroneous solu-
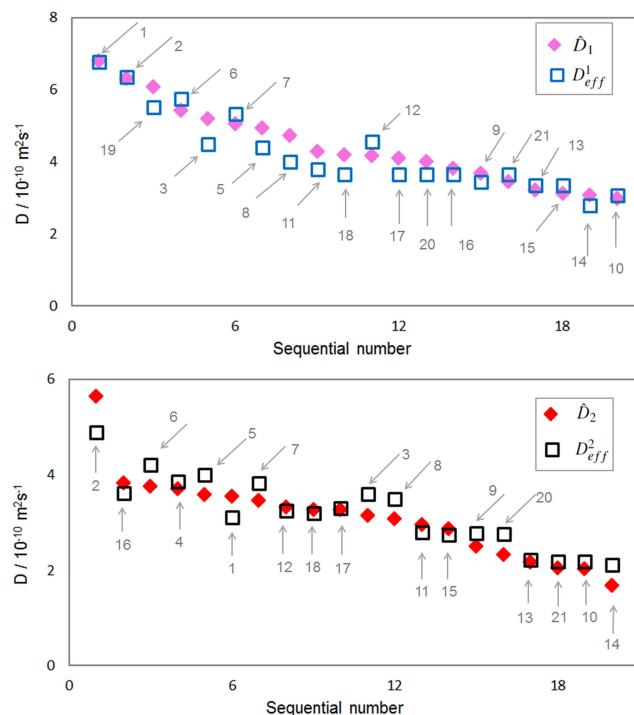
Fig. 9 Comparison of the eigenvalues with effective (quasi-binary) diffusion coefficients: (top) eigenvalue $\hat{D}_1$ and D^1_{pbin} obtained for the signal with the injection $\Delta c_2 = 0$; (bottom) eigenvalue $\hat{D}_2$ and D^2_{pbin} obtained for the signal with the injection $\Delta c_1 = 0$. Horizontal axes indicates to sequential number after sorting eigenvalues from the largest to the smallest value. The arrows with numbers in the figure indicate labeling of the points according to Fig. 2.
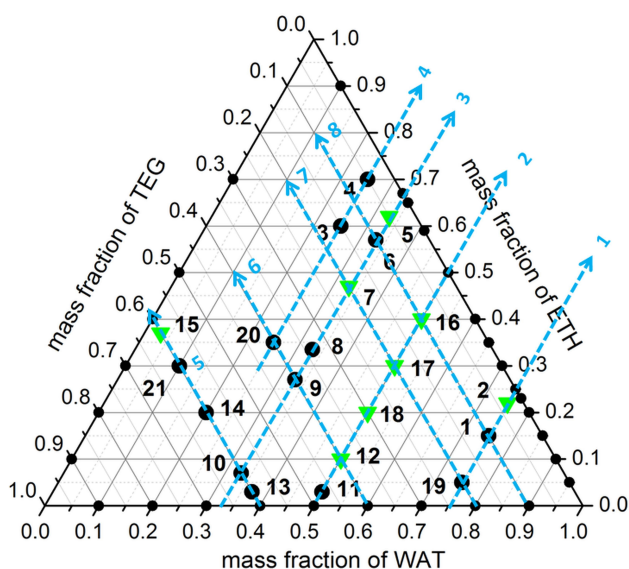
Fig. 10 Paths indicating the sequence of the determination of diffusion coefficients. The fitting was performed in the direction of arrows as well as in opposite direction. Green triangles indicate the points at which the Gaussian dispersion peaks without dips were observed.

tions.

Next, the ternary mixture is considered to be pseudo-binary; subsequently, the dispersion peak is characterized by a single diffusion coefficient, referred to as the pseudo-binary diffusion coefficient D_{pbin}. The quasi-binary diffusion coefficients can be identified for each species pair in the mixture. Two effective coefficients, D^1_{pbin} and D^2_{pbin}, were determined in each point which corresponds to injections with $\Delta c_2 = 0$ and $\Delta c_1 = 0$ respectively. The injections when both concentrations change, i.e., $\Delta c_1 \neq 0$ and $\Delta c_2 \neq 0$, result, as a rule, in a peak with dips and they were not considered. Figure 9 allows the detailed quantitative comparison between the eigenvalues $\hat{D}_i$ of the diffusion matrix and D^i_{pbin}. For a better appreciation the $\hat{D}_i$ were sorted from the largest to the smallest value and the horizontal axis indicates sequential numbers after sorting. The basis of our understanding is that the slowest kinetic, i.e., smallest eigenvalue defines the overall temporal evolution of the diffusion process. Interestingly, smallest eigenvalues $\hat{D}_2$ satisfactory correlate with D^1_{pbin} but the largest eigenvalues $\hat{D}_1$ also satisfactory correlate with D^2_{pbin}. This finding has significant implications for guiding the efforts to select the correct solution and also provides a hint for the choice of the starting set of parameters.

The convergence of the fitting routine depends on the initial guess and its sensitivity increases when approaching the binary limits. To minimize the influence of the initial guess, the fitting is consecutively performed following several paths starting closely to the binary mixture water-TEG. The direction of the eight paths followed during the fitting is indicated by arrows in Fig. 10. The values of the diffusion coefficients along the paths directed to the left and right sides were thoroughly verified in the points of intersection. When approaching the binary mixture on the bottom, the cross diffusion coefficient D_{21} tends towards zero whereas D_{11} reaches the limit of the binary diffusion coefficient in the

water-TEG mixture. Indeed, the mass flux of ethanol and its concentration tend to zero, i.e. $j_2 \to 0$ and $\Delta c_2 \to 0$. Then from eqn (2) it follows that $D_{21} \to 0$ and from eqn (1) it follows that $D_{11} \to D_{WAT-TEG}$. Note that the behavior of D_{22} and D_{12} cannot be predicted from this analysis.

At the other end of the concentration path, e.g., on the left hand side in Fig. 10, the mass flux of water and its concentration tend to zero, i.e. $j_1 \to 0$ and $\Delta c_1 \to 0$. Then from eqn (1) it follows that $D_{12} \to 0$ and from eqn (2) follows that $D_{22} \to D_{ETH-TEG}$. Again, the behavior of the two other coefficients D_{11} and D_{21} cannot be predicted from this analysis. However we used this asymptotic only for path 5.

The asymptotic behavior on the right hand side in Fig. 10, i.e., when $c_3 = c_{TEG} \to 0$, with our choice of the reference component does not allow a similar interpretation via the simple analysis of the mass fluxes in eqns (1)-(2). A more detailed analysis published elsewhere has shown that[44]

$$D_{22} - D_{21} \xrightarrow{c_3 = c_{TEG} \to 0} D_{WAT-ETH}.$$
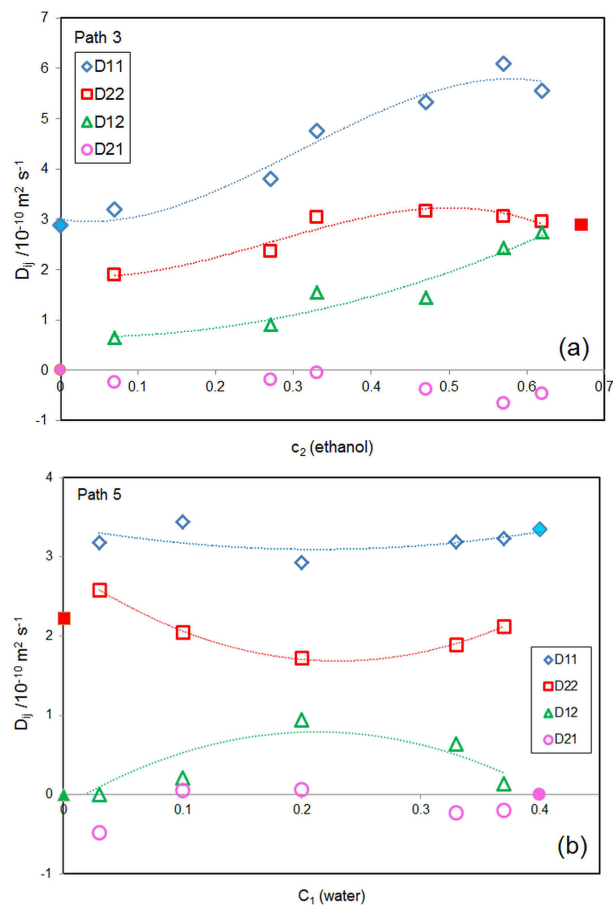
Fig. 11 Fickian diffusion coefficients D_{ij} along right and left directed concentration paths in the ternary system water-ethanol-TEG (a) path 3 when mass fraction of water is kept constant $c_1 = 0.33$; (b) path 5 when mass fraction of TEG is kept constant $c_3 = 0.4$. The filled symbols indicate asymptotic values approaching the binary subsystems. The dotted trend lines are given as the guidance for eyes.

Table 6 Compositions of ternary mixtures in mass fractions, diffusion coefficients $D_{ij}/10^{-10}$ and eigenvalues of the diffusion matrix $\hat{D}_i/10^{-10}$. First column indicates the point number in Fig. 2 and S_R is the used sensitivity ratio. $T = 298$ K

N	water mass fr.	ethanol mass fr.	TEG mass fr.	S_R	D_{11} m^2s^{-1}	D_{12} m^2s^{-1}	D_{21} m^2s^{-1}	D_{22} m^2s^{-1}	$\hat{D}_1$ m^2s^{-1}	$\hat{D}_2$ m^2s^{-1}
1	0.75	0.15	0.10	0.860	5.84	-1.90	-0.83	4.69	6.65	3.88
2	0.75	0.22	0.03	0.834	6.05	-0.97	-0.11	5.90	6.31	5.64
3	0.25	0.60	0.15	0.418	6.41	4.07	-0.99	1.91	5.18	3.14
4	0.25	0.70	0.05	0.417	6.37	0.62	-0.35	3.62	6.29	3.70
5	0.33	0.62	0.05	0.459	5.56	2.74	-0.46	2.95	4.93	3.58
6	0.33	0.57	0.10	0.451	6.10	2.40	-0.66	3.07	5.42	3.75
7	0.33	0.47	0.20	0.473	5.33	1.45	-0.37	3.16	5.04	3.44
8	0.33	0.33	0.33	0.482	4.76	1.55	-0.04	3.03	4.72	3.07
9	0.33	0.27	0.40	0.488	3.80	0.91	-0.18	2.36	3.67	2.49
10	0.33	0.07	0.60	0.521	3.19	0.64	-0.23	1.90	3.06	2.03
11	0.50	0.03	0.47	0.705	4.14	-0.81	-0.22	3.10	4.29	2.95
12	0.50	0.10	0.40	0.673	4.04	-0.64	-0.13	3.43	4.16	3.32
13	0.37	0.03	0.60	0.514	3.24	0.14	-0.20	2.13	3.21	2.16
14	0.20	0.20	0.60	0.423	2.94	0.94	0.06	1.72	2.98	1.68
15	0.03	0.37	0.60	0.608	3.18	0.04	-0.48	2.79	3.12	2.85
16	0.50	0.40	0.10	0.562	3.99	-0.70	0.04	3.65	3.82	3.82
17	0.50	0.40	0.10	0.590	4.20	0.34	-0.31	3.15	4.09	3.26
18	0.50	0.20	0.30	0.629	4.11	-0.26	-0.29	3.35	4.19	3.26
19	0.75	0.05	0.20	0.925	5.99	-3.98	-0.02	5.01	6.08	4.93
20	0.25	0.35	0.40	0.435	5.02	4.41	-0.63	1.29	4.00	2.31
21	0.10	0.30	0.60	0.358	3.44	0.21	0.06	2.05	3.45	2.04

3.2.3 Diffusion coefficients

We proceed now with the analysis of the diffusion coefficients in the ternary mixture water-ethanol-TEG obtained by the Taylor dispersion measurements. Over the entire concentration space the system did not reveal a sharp change of the coefficients. We begin our study by considering variations of four diffusion coefficients along paths 3 and 5 shown in Fig. 11. The filled symbol of the same type as the open ones indicate the asymptotic value of the coefficient approaching a binary subsystem. Along path 3 in Fig. 11(a) (concentration of water is kept constant) the cross coefficient D_{21} is close to zero over the entire path while all other coefficients slowly grow departing from the bottom side. On this path our measurements perfectly meet the expectations on both binary limits. Along path 5 in Fig. 11(b) (concentration of TEG is kept constant) variations of coefficients are also rather smooth. Again, the cross diffusion coefficient D_{21} is close to zero over the entire path while another cross diffusion coefficient D_{12} tends to zero only at the binary limits. The measured coefficients along path 5 are consistent with the asymptotic values; the less good agreement occurs for the coefficient D_{22} approaching to the binary system ethanol-TEG.

The maps of Fickian diffusion coefficients and eigenvalues of the diffusion matrix are shown in Fig. 12. It is important to note that the color scale at each triangle is different because the variation amplitude of each quantity is different. The map for D_{11} occupies a larger area in the concentration space than any other quantity, because the binary subsystem water-triethylenglycol was comprehensively measured (see Fig. 5) and from the analysis of mass fluxes it follows that $D_{11} \rightarrow D_{WAT-TEG}$. Additionally, there is a sufficient number of ternary points in the vicinity of the binary boundary. Consequently, on the bottom of the triangle we match coefficients for ternary and binary mixtures. The main coefficients D_{11} and D_{22} are almost constant in a large region around the symmetric point, the point where $c_1 = c_2 = c_3$. Both coefficients grow when approaching the right corner, where the mixture is rich in water and poor in ethanol and TEG. On the opposite side, i.e., at the left corner, where the mixture is poor in water and ethanol and rich in TEG, both coefficients decrease. Moreover, D_{11} attains its minimal value at this corner. Their behavior diverges in the upper part of the triangle. A noteworthy result of the study is that in all measured points the main coefficients are positive and have the same order of magnitude $\sim O(10^{-10} \text{ m}^2/\text{s})$. In the fitting procedure we did not impose any restrictions on the sign of the diffusion coefficients.

The behavior of cross diffusion coefficients D_{12} and D_{21} is very different. As a rule D_{21} is negative and smaller than D_{12} by an absolute value. Furthermore, D_{21}, is at least one order of the magnitude smaller than the main coefficients almost within the entire composition triangle. It grows when approaching the binary subsystem water-ethanol. On the contrary, D_{12} is mostly positive over the concentration space. However, it becomes strongly negative in the right corner, where the mixture is rich in water and poor in ethanol. Note that the shape of dispersion peaks in these corner points, i.e. points 1 and 19, display broadening. These results confirm the hypothesis of Price[29] that such peak shape is due to a large and negative value of D_{12}.

The maps of eigenvalues $\hat{D}_1$ and $\hat{D}_2$ are different with respect to the locations of maxima and minima. Their concentration dependence looks as smooth as that of the individual coefficients.
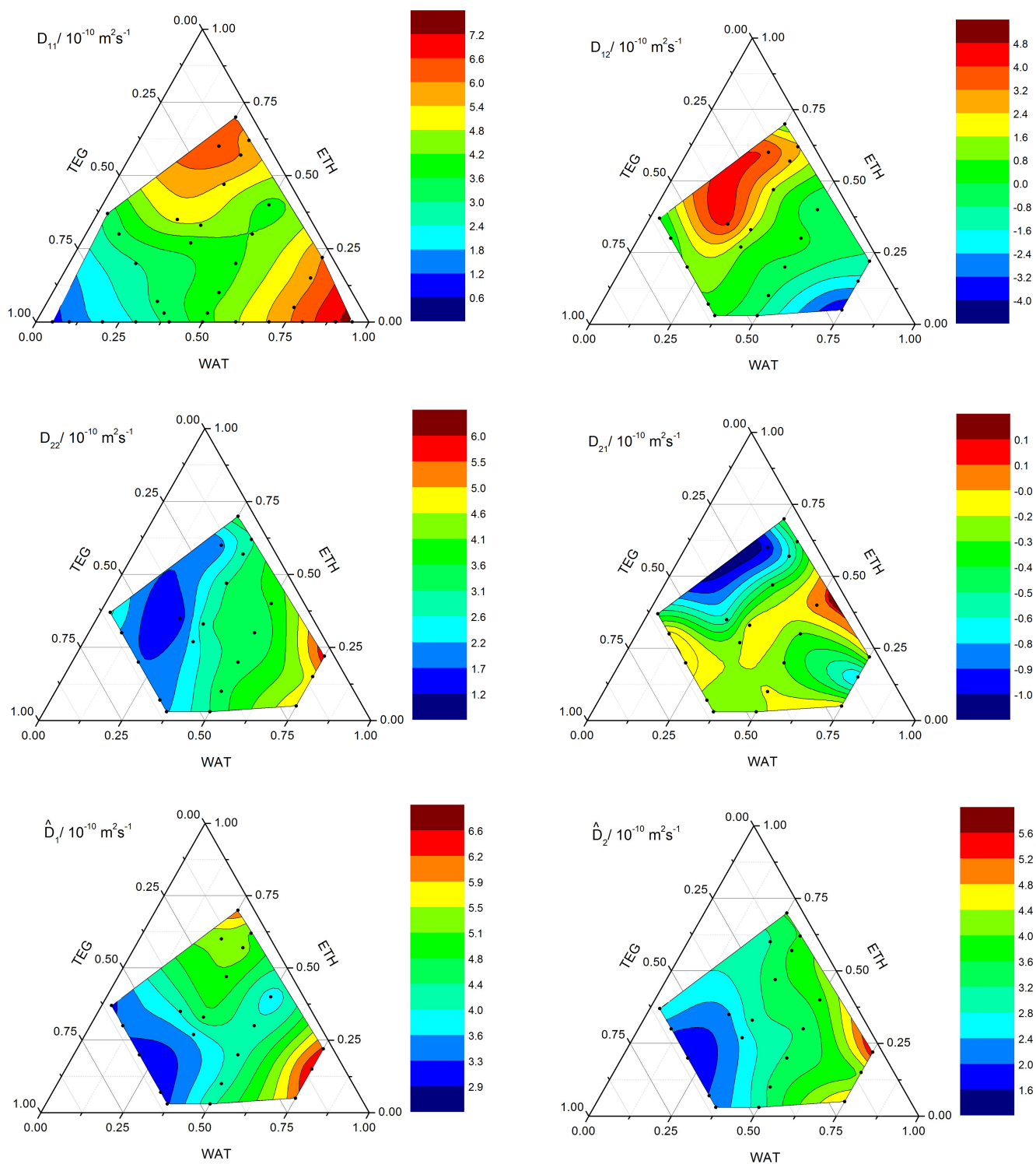
Fig. 12 Fickian diffusion coefficients D_{ij} and eigenvalues $\hat{D}_i$ over measured concentration space in the ternary system water (WAT)-ethanol (ETH)-triethylenglycol (TEG). The concentration is expressed in mass fraction units. Color scales indicate the variation amplitude the quantities. Small dots indicate experimental points.

We did not notice any visible correlation between eigenvalues and main coefficients of the diffusion matrix. It should be only pointed out that the ratio of eigenvalues $\hat{D}_1/\hat{D}_2$ lies between 1 and 2: it is very close to unity at the point 16 and tends to two in the region poor in water, i.e., $c_1 < 0.2$

Quantitative results for the diffusion coefficients measured by Taylor dispersion in the ternary mixtures are listed in Table 6. Note, that in the numbering of the points there is no special order except a chronological one. In addition to the diffusion coefficients we also provide the sensitivity ratio S_R obtained via refractive indices[31]. The data in Table 6 indicate mean values while the standard deviation is about 3-6%.

4 Conclusions

We have performed a comprehensive study of the Fickian diffusion coefficients in the ternary liquid mixture water-ethanol-triethylene glycol and its binary subsystems at $T = 298$ K. The mutual diffusion coefficients in 30 binary mixtures were measured using the Optical Beam Deflection and the Taylor dispersion technique and results were favorably compared with literature data when they are available. For the two dilute limits $c \rightarrow 1$ and $c \rightarrow 0$ the binary diffusion coefficients were estimated from the Stokes-Einstein equation using both slip and stick boundary conditions. In all cases these estimations are in reasonable agreement with the extrapolations of the measured diffusion coefficients.

The diffusion coefficient in the ternary mixture was consistently measured by means of the Taylor dispersion technique for 21 compositions along eight paths corresponding to constant concentrations of either water or triethylene glycol. The measurements revealed that over the entire concentration space the main diffusion coefficients smoothly vary in the range $(1.3 - 5.9) \cdot 10^{-10}$ m^{2}s^{-1} and that one of them is always larger than the other one, $D_{11} > D_{22}$. It was demonstrated that for the associated ternary mixture the off-diagonal elements of the diffusion matrix cannot be omitted. In particular, D_{12} varies in the same range as the main elements while D_{21} displays a trend to be one order of the magnitude smaller than the other coefficients.

Additionally, we have found that the pseudo-binary diffusion coefficients correlate well with the eigenvalues in injections when either c_1 or c_2 are kept constant. On the contrary, the experimental results did not confirm previous theoretical predictions[45] that the pseudo-binary diffusion coefficients approximate to the main elements of the diffusion matrix.

Acknowledgements

References

1 P. W. M. Rutten, Diffusion in Liquids. Delft University Press, Delft (1992)

2 K.C. Pratt, W.A. Wakeham, *Proc. R. Soc. Lond. Ser. A–Math. Phys. Sci.*, 1974, **336**, 393.

3 D. G. Leaist, *J. Phys. Chem.* 1990, **94**, 5180.

4 J. F. Torres, A. Komiya, E. Shoji, J. Okaji, and S. Maruyama, *Opt. Lasers Eng.*, 2012, **50**, 1287.

5 A. Mialdun, V. Yasnou, and V. Shevtsova, *C. R. Mec.*, 2013, **341**, 462.

6 D. Alonso De Mezquia, M. M. Bou-Ali, M. Larranaga, J. A. Madariaga, and C. Santamaría, *J. Phys. Chem. B*, 2012, **116**, 2814.

7 M. Klein and S. Wiegand, The Soret effect of mono-, di- and tri-glycols in ethanol, *Phys. Chem. Chem. Phys.*, 2011, **13**, 7090.

8 M. Gebhardt, W. Köhler, A. Mialdun, V. Yasnou and V. Shevtsova, *J. Chem. Phys.,* 2013, **138**, 114503.

9 A. Mialdun, V. Yasnou, V. Shevtsova V, A. Königer, W. Köhler, D. Alonso de Mezquia, M.M. Bou-Ali, *J. Chem. Phys.*, 2012, **136(24)**, 244512.

10 A. Königer, B. Meier, and W. Köhler, *Philosophical Magazine*, 2009, **89(10)** , 907.

11 P. Polyakov and S. Wiegand, *Phys. Chem. Chem. Phys.*, 2009, **11**, 864.

12 Y. Kishikawa, H. Shinohara, K. Maeda, Y. Nakamura, S. Wiegand and R. Kita, *Phys. Chem. Chem. Phys.*, 2012, **14**, 10147.

13 J. Wambui Mutoru and A. Firoozabadi, *J. Chem. Thermodynamics*, 2011, **43**, 1192.

14 R. Taylor and R. Krishna, *Multicomponent Mass Transfer*, Wiley, **1993**.

15 A. Alizadeh, C. A. N. de Castro and W. A. Wakeham, *Int. J. Thermophys.*, 1980, **1(3)**, 243.

16 A. Mialdun and V. Shevtsova, *J. Chem. Phys.*, 2013, **138**, 161102.

17 M. Gebhardt and W. Köhler, *J. Chem. Phys.*, 2015, **142**, 084506.

18 A. Mialdun, V. Sechenyh, J. C. Legros, J. M. Ortiz de Zárate, and V. Shevtsova *J. Chem. Phys.*, 2013, **139**, 104903.

19 M. Larrañaga, D. A. S. Rees, and M. Mounir Bou-Ali, *J. Chem. Phys.*, 2014, **140**, 054201.

20 A. Königer, H. Wunderlich and W. Köhler, *J. Chem. Phys.*, 2010, **132** 174506.

21 H.T. Cullinan Jr., *Ind. Eng. Chem. Fundam.*, 1965, **4**, 133.

22 A. Mialdun, J.C. Legros, V. Yasnou, V. Sechenyh and V. Shevtsova, *Eur. Phys. J. E*, 2015, **38**, 27

23 V. Shevtsova, Y. A. Gaponenko, V. Sechenyh, D. E. Melnikov, T. Lyubimova and A. Mialdun, *J. Fluid Mech.*, 2015, **767** 290.

24 A. Mialdun, C. Minetti, Y. Gaponenko, V. Shevtsova and F. Dubois, *Microgravity Sci. Technol.*, 2013, **25**, 83.

25 M.M. Bou-Ali, A. Ahadi, D. Alonso de Mezquia, Q. Galand, M. Gebhardt, O. Khlybov, W. Köhler, M. Larrañaga, J.C. Legros, T. Lyubimova, A. Mialdun, I. Ryzhkov, M.Z. Saghir, V. Shevtsova and S. Van Vaerenbergh, *Eur. Phys. J. E*, 2015, **38**, 30.

26 S. Pařez, G. Guevara-Carrion, H. Hasseb and J. Vrabec, *Phys.Chem. Chem. Phys.*, 2013, **15**, 3985.

27 V. Sechenyh, J.C. Legros and V. Shevtsova, *C. R. Mec.*, 2013, **341**, 490.

28 G.B. Ray and D. Leaist, *J. Chem. Eng. Data* 2010, **55**, 1814.

29 W. E. Price, *J. Chem. Soc.Faraday Trans. I*, 1988, **84(7)**, 2431.

30 D. G. Leaist, *J. Chem. Soc. Faraday Trans.*, 1991, **84(4)** 597.

31 V.V. Sechenyh, J.C. Legros and V. Shevtsova, *J. Chem. Thermodynamics*, 2011, **43**, 1700.

32 V. V. Sechenyh, J.C. Legros and V. Shevtsova, *J. Chem. Eng. Data*, 2012, **57**, 1036.

33 V.V. Sechenyh, J.C. Legros and V. Shevtsova, *J. Chem. Thermodynamics*,(2013), **62** 64.

34 G. Wittko and W. Köhler, *Philos. Mag.*, 2003, **83**, 1973.

35 A. Becker, W. Köhler, and B. Müller, *Ber. Bunsenges. Phys. Chem.*, 1995, **99**, 600.

36 G. Wittko and W. Köhler, *Eur. Phys. J. E*, 2006, **21**, 283.

37 M. Giglio, A. Vendramini, *Phys. Rev. Lett.*, 1975, **34**, 561.

38 R. Piazza, A. Guarino *Phys. Rev. Lett.*, 2002, **88**, 208302.

39 B. R. Hammond and R. H. Stokes, *Trans. Faraday Soc.*, 1953, **49**, 890.

40 K. R. Harris, T. Goscinska, H. N. Lam, *J. Chem. Soc. Faraday Trans.*, 1993, **89**, 1969.

41 P. Kolodner, H. Williams, C. Moe, *J. Chem. Phys.*, 1988, **88**, 6512.

42 S. Wiegand, H. Ning, H. Kriegs, *J. Phys. Chem. B*, 2007, **111**, 14169.

43 G. Heuberger, H. Sillescu, *J. Phys. Chem.*, 1996, **100**, 15255.

44 V.V. Sechenyh, J. C. Legros, A. Mialdun, J. M. Ortiz de Zárate and V. Shevtsova *J. Phys. Chem.*, submitted, 2015.

45 L.O. Sundelöf, *J. Chem. Soc., Faraday Trans.2*, 1981, **77**, 1779.

46 J. Wambui Mutoru, A. Leahy-Dios, A. Firoozabadi, *AIChE J.*, 2011, **57**, 1617.

47 C. R. Wilke, P. Chang, *AIChE J.*, 1955, **1**, 264.

48 L. Paduano, R. Sartorio, G. D'Errico and V. Vitagliano, *J. Chem. Soc., Faraday Trans.*, 1998, **94 (17)**, 2571.